Available online at www.sciencedirect.com
ScienceDirect
Composites Science and Technology 67 (2007) 3090–3097
COMPOSITES SCIENCE AND TECHNOLOGY
www.elsevier.com/locate/compscitech

Hygromechanical properties of composites of crosslinked allylglycidyl-ether modified starch reinforced by wood fibres

Jie Duanmu [a], E. Kristofer Gamstedt [b], Ari Rosling [a,*]

[a] Laboratory of Polymer Technology, Åbo Akademi University, Biskopsgatan 8, FIN-20500 Åbo, Finland
[b] Department of Solid Mechanics, Royal Institute of Technology (KTH), Osquars backe 1, SE-100 44 Stockholm, Sweden

Received 1 September 2006; received in revised form 25 April 2007; accepted 30 April 2007
Available online 18 May 2007

Abstract

In a previous work a new family of thermoset composites of allylglycidyl ether modified starch as matrix, an ethylene glycol dimethacrylate as cross-linker and a wood fibre as reinforcement were prepared. The aim of the present work was to study the hygromechanical properties of the new composites including density, dimensional stability in water, water uptake, stiffness, and ultimate strength in three-point bending. It was shown that the samples with a starch matrix of a high degree of substitution (DS = 2.3), HDS, absorbed less water, were more stable in water and had also higher stiffness and strength than corresponding composite samples with a starch matrix of low degree of substitution (DS = 1.3), LDS. Overall, the fibre addition improved water stability. An increased fibre content from 40 to 70% by weight had a negligible impact on the water uptake. An increase in fibre content did, however, improve the mechanical properties. The HDS-sample with highest fibre content, 70% by weight showed the highest Young's modulus (3700 MPa) and strength (130 MPa), which are markedly higher compared with the samples based on the pure HDS matrix (Young's modulus of 360 MPa and strength of 15 MPa). The measured Young's modulus and tensile strength values were roughly one order of magnitude higher than earlier reported cellulosic fibre reinforced natural polymer composites.

Keywords: A. Wood; B. Hygrothermal effect; D. Fractography; E. Casting; Cross-linked starch

1. Introduction

Biocomposites composed of biodegradable polymers as matrix and biofibres as reinforcement has attracted extensive attention due to their favourable properties and from the viewpoint of protection of the natural environment in recent years [1,2]. Biofibre reinforced polymers are characterized by their low cost, low density, high specific stiffness and strength, biodegradability, and good mechanical properties [1,2]. An important drawback of biofibres is their hydrophilic nature which lowers the compatibility with hydrophobic polymeric matrix during composite fabrication [2]. A variety of natural fibre reinforced biocomposites have been synthesized from renewable and natural polymers [1–13]. However, until now, the biodegradable composites cannot be widely applied, because of their limitations in prices or properties compared to plastics of petroleum origin.

Among the natural polymers, starch has been considered as one of the most promising materials for biodegradable plastics, because of its natural abundance and low cost. Starch is the major carbohydrate in plant stem and seed endosperm, where it is found as granules. However, starch-based plastics have some drawbacks, including poor long-term stability caused by the water absorption, poor mechanical properties and processability. Effective ways to overcome some of these drawbacks are chemical modification of starch [14], grafting of synthetic polymers onto starch [15–17] and blending starch with synthetic polymers as plasticizers [18–23]. In addition, thermoplastic starch composites with improved mechanical properties have been achieved by addition of cellulosic fibres [24].

* Corresponding author. Tel.: +358 2 2154236; fax: +358 2 2154866.
E-mail address: ari.rosling@abo.fi (A. Rosling).

0266-3538/$ - see front matter © 2007 Elsevier Ltd. All rights reserved.
doi:10.1016/j.compscitech.2007.04.027

In the previous work [25] we synthesized and prepared, composites obtained from a allylglycidyl-ether (AGE) modified starch as matrix, a ethylene glycol dimethacrylate (EGDA) as cross-linker and a wood fibre as reinforcement. The main objective of this work is to evaluate the hygromechanical properties of the composites in terms of Young's modulus and ultimate strength in a three-point bending test, study the water absorption behaviour and the interface between the matrix and fibres.

2. Experimental procedures

2.1. Material

Native potato starch was received as a gift from Lyckeby Stärkelse, Sweden. Bleached kraft softwood pulp fibres was supplied by Imatra mill of StoraEnso.

Preparation of composites obtained from allylglycidyl-ether modified starch as matrix, a EGDA as cross-linker and a wood fibre as reinforcement is reported in a previous work [25]. Composites of two different matrices, i.e. starch with a low degree of substitution of AGE (DS = 1.3), denoted LDS-x, and a starch with a high degree of substitution (DS = 2.3), denoted HDS-y, with different fibre contents, x and y in % by weight, were used in the present study. The fibre length and width distributions of pure bleached softwood fibre samples was measured by Kajaani Fiberlab (Metso Automation) fibre length analyzer. The fibre length shows a considerable scatter (rough average 2 mm) and the measured average fibre diameter was 20–30 μm, thus the fibres can be considered long and slender, with an aspect ratio of approximately 100. Fibre degradation during processing can be neglected, since the fibres were treated gently during manufacture of the composites.

2.2. Interface and fibre dispersion

Composite samples were broken into half and the fracture surfaces were viewed with LEO 1530 SEM (scanning electron microscope) working at an accelerating voltage of 15 kV. Several composite samples were embedded in epoxy resin, cut at the middle and the cross-sections were polished with successively finer silicon carbide papers up to 2400 grit. The fibre dispersion inside the composite was studied from the polished cross-sections with SEM.

2.3. Density

Excluding the lumen, soft wood fibres have a reported density of 1500 kg/m^3 [26]. This value was used when estimating the density of the composites and the volume fractions of the constituents.

2.4. Water absorption and dimensional stability

For the water uptake analysis, three disk-shaped samples (12 mm × 3 mm) of each composite LDS-40, LDS-60, HDS-0, HDS-40 and HDS-60 conditioned at ambient environment (25 °C, relative humidity 65 ± 5%) for 1–2 weeks were weighed for their reference weight, and placed into separate test tubes filled with ordinary tap water (10 ml) at room temperature. At predetermined points of time, the selected samples were removed from the water solution and their weight was measured. Immediately before weighing, the surface of the samples were wiped with a tissue that absorbed the superficial free water. Five locations on each sample surface were selected to measure the thickness variation with increasing time. Simultaneously, the diameter increase with time was also measured for four positions. The average values of the dimensions and weight increase as a function of time of three specimens were calculated.

The hygroexpansion coefficients in the thickness direction β_z and in the radial direction β_r are calculated from the dimensional changes caused by a change in moisture content, Δm:

$$\beta_z = \frac{\varepsilon_z}{\Delta m} \tag{1}$$

$$\beta_r = \frac{\varepsilon_r}{\Delta m} \tag{2}$$

where ε_z is the strain in the thickness direction, and ε_r is the strain in radial direction.

The diameter of oblate cylindrical specimens was much larger than their thickness. If the diameter to thickness ratio is assumed to be much larger than the ratio between the estimated diffusion (i.e. effective values) coefficients of the radial and thickness directions, the moisture transport in the samples can be regarded as one-dimensional Fickean diffusion. The estimated diffusion coefficient (i.e. effective value) D in the thickness direction was calculated from the moisture content variation of the initial linear part of the curve when the water content is studied as a function of time, e.g. [27]:

$$D = \frac{\pi l_z}{16 m_\infty^2} \frac{m_2 - m_1}{\left(t_2^{1/2} - t_1^{1/2}\right)^2} \tag{3}$$

where l_z is the average thickness of the wet-sample at t_1 and t_2, m_∞ is absorbed water content at saturation, m_1 and m_2 are absorbed water contents at corresponding time points t_1 and t_2, respectively.

2.5. Mechanical properties

Six rectangular bars (12 mm × 3 mm × 3 mm) of each composite, namely LDS-40, LDS-60, HDS-40, HDS-60 and HDS-70, were manufactured. The machined surfaces were polished with 1600 grit silicon carbide paper. The test samples were conditioned at ambient environment (25 °C, relative humidity 65 ± 5%) for 1 week before mechanical testing. Three specimens each was subjected to a three-point bending test in the in-plane direction and the out-of-plane direction, respectively (see Fig. 6). A Minimat 2000 micro-tensile machine was used with a 200 N load cell. In addition, three rectangular bars (12 mm × 6 mm × 3 mm) of neat

HDS-0 were tested in the same load cell. Samples of LDS-60 and HDS-60 were immersed in water at room temperature for 24 h (close to saturation), and subsequently tested in both in-plane and out-of-plane directions with a 20 N load cell.

The in-plane Young's modulus was calculated according Timoshenko beam theory with the following formula [28]:

$$E = \frac{1}{C_b}\left[\frac{1}{4b}\left(\frac{L}{h}\right)^3 + \frac{\beta(1+v)}{2b}\frac{L}{h}\right] \quad (4)$$

where $1/C_b$ is the slope of the linear part of the load versus midpoint deflection curves, b is the width of specimen, h is the height of specimen, L is the distance between the end supports, v is the Poisson's ratio assumed to be 0.3, and β is geometrical factor assumed to 1.2 for rectangular cross-sections.

The ultimate strength σ was calculated from the three-point bending test as

$$\sigma = \frac{M}{I}\frac{h}{2} \quad (5)$$

where maximum moment is

$$M = \frac{PL}{4} \quad (6)$$

and the second moment of area is

$$I = \frac{bh^3}{12} \quad (7)$$

P is the applied load, h is the height of the specimen, and b is the width of the specimen.

3. Results and discussion

3.1. Interface and fibre dispersion

The mould-face and fracture surface of HDS and LDS composites and the fibre dispersion in HDS-composites are shown in SEM micrographs in Fig. 1a–d. The outer surface of HDS-composite appears to be smooth and flawless whereas the LDS composite surface includes areas where the matrix has not been able to flow out and wet the underlying fibres close to the surface. This phenomenon is probably due to a higher melt viscosity of the LDS matrix and possibly too fast curing thus inhibiting the matrix flow. Fractographic investigations of both types of composites, i.e. LDS and HDS in Fig. 1b and d, respectively, showed cohesive failure with relatively intact fibre–matrix bonds, where the wood fibres were split into sprawling fibrils.

The composite fracture surfaces reveal a good wetting of the fibres by the modified starch matrix. In both composites the fibres are tightly surrounded by the starch matrix, constituting a nonporous compact matrix and very little fibre pull-out is visible. The fibre–matrix compatibility is also detectable in the composite density values (Table 1). The diameter and thickness of oblate cylindrical specimens was measured with micrometer and the density of composites

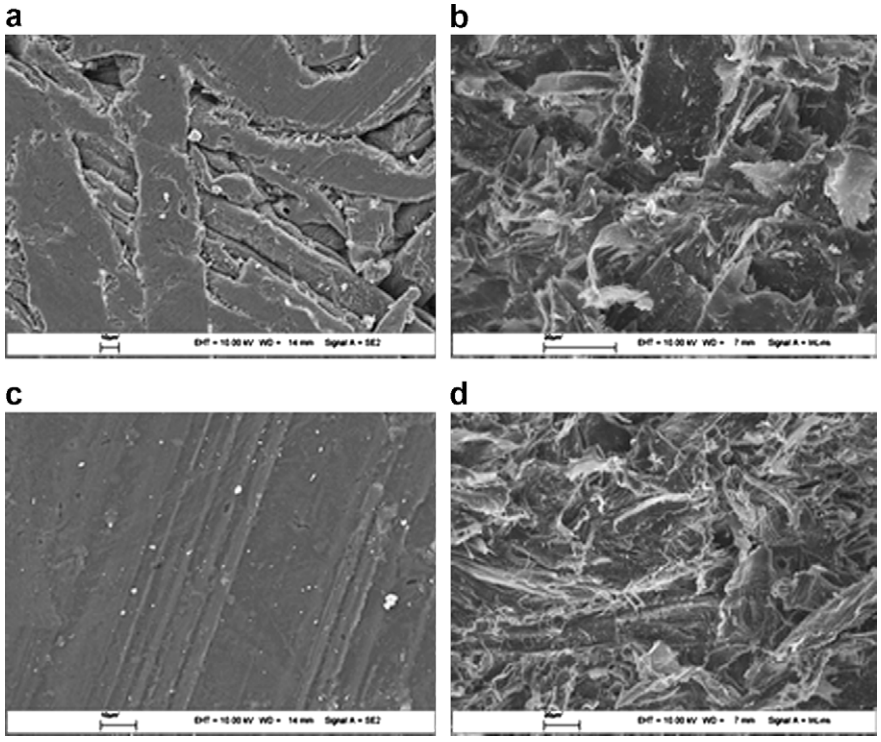

Fig. 1. SEM images of LDS-60 composite at (a) the mould-face surface with 500× magnification, at (b) a fracture surface with 1000× magnification, and of HDS-60 composite at (c) the mould-face surface with 1000× magnification, and at (d) a fracture surface with 500× magnification.

Table 1
Composite densities

Specimen	Density (kg/m^3)	Standard deviation (kg/m3)
Softwood fibre	1500[a]	–
LDS-0	1310[b]	–
LDS-40	1388	7.9
LDS-60	1427	17.8
HDS-0	1232	11.7
HDS-40	1311	43.2
HDS-60	1389	11.2
HDS-70	1429	10.1

[a] General value given for collapsed softwood fibres.
[b] Calculated value from the rule of mixtures, Eq. (8).

was determined by method of weight and dimensions. The density follows reasonably well the rule of mixtures for the HDS-composites. The composite density ρ_c is expressed as

$$\rho_c = w_f\rho_f + w_m\rho_m \quad (8)$$

where ρ_f and ρ_m are the densities of the fibres and matrix, respectively, and w_f and w_m are their respective weight fractions, assuming no voids. For the unreinforced LDS starch, the density was estimated from extrapolation of the rule of mixtures in Eq. (8). A poor matrix–fibre compatibility would obviously create inferior interface bonding with the formation of voids between them and thus reducing the density.

The SEM images of polished cross-sections in Fig. 2 of HDS-composites show a good fibre dispersion and excellent wetting of the fibres. In addition, the HDS matrix has even been able to penetrate trough the cell walls filling up the lumen of uncollapsed latewood fibres. The high fibre content in the HDS-60 composite has apparently caused a substantial amount of fibres to collapse and flatten. There are also some minor cracks noticeable in the matrix between fibres in the HDS-60 composite. These cracks can originate from residual stresses formed during manufacturing.

The uniform mixing and processing conditions, where the pressure was applied in one direction onto the flat specimens, suggest that the fibres have virtually random in-plane orientation distribution. This was corroborated by cross-sectional microscopy viewed in different directions. The fibres were observed to have no preferential orientation in the plane, and almost no fibres had an out-of-plane orientation.

3.2. Water absorption and dimensional stability

The intrinsic hydrophilicity of starch-based materials is a major concern and drawback in many practical applications. In most cases a direct immersion of the starch product in water would mean a direct end to its functionality. In the present study initial samples were conditioned at ambient conditions at 65 ± 5% relative humidity at 25 °C for 1 week before immersion in water. Figs. 3–5 show the water uptake, changes in sample diameter and thickness as a function of time. The modifications of the starch matrix, i.e. LDS or HDS, had a great impact on the resistance to water uptake of the composites. The LDS matrix confers a greater hydrophilicity due to a lower degree of AGE substitution. Thus, composites of LDS show markedly higher water absorption at saturation (31%) compared with corresponding HDS composites (14–18%) (see Table 2). The saturation level (approximately 95% of the predicted asymptotic value) for cylindrical samples was reached in

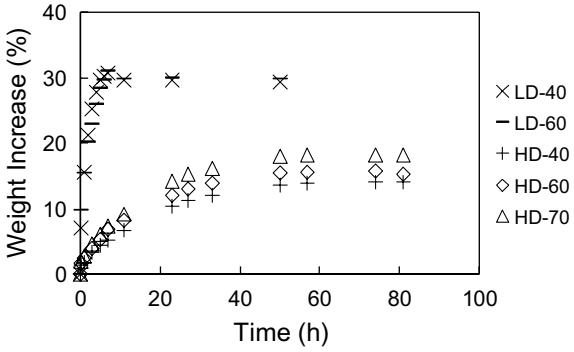

Fig. 3. Weight increase of LDS and HDS-composites with immersion time in water.

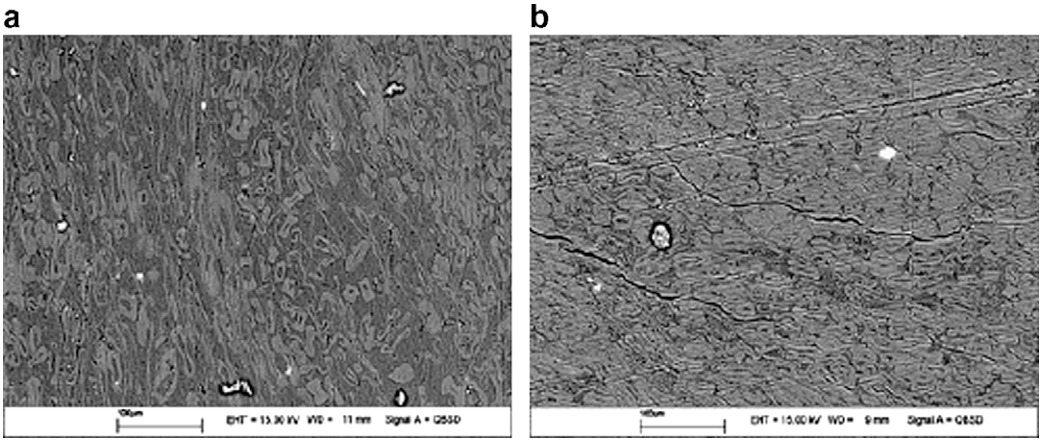

Fig. 2. Polished cross-sections of (a) HDS-40 and (b) HDS-60 composites. The scale bars indicate 100 μm.

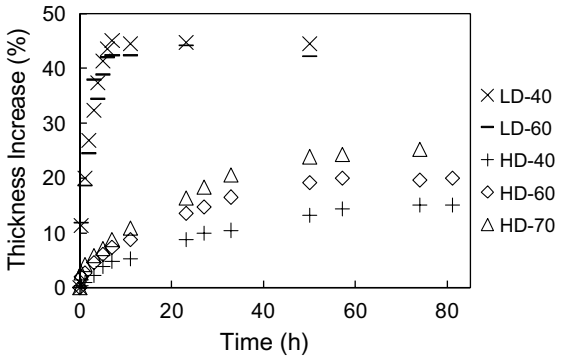

Fig. 4. Thickness increase of LDS and HDS-composites (out-of-plane hygroscopic strain) with immersion time in water.

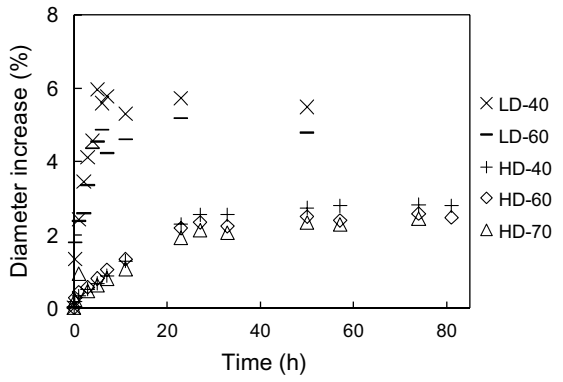

Fig. 5. Diameter increase (in-plane hygroscopic strain) with immersion time in water of flat cylindrical specimens of LDS and HDS-composites.

Table 2
One-dimensional estimated diffusion (i.e. effective value) coefficient D, hygroexpansion coefficient β in the out-of-plane z-direction and the in-plane radial direction r, and moisture content at saturation m_∞

Property (unit)	LDS matrix Fibre content (w%)		HDS matrix Fibre content (wt%)		
	40	60	40	60	70
D (mm^2/h)	0.35 (0.12)	0.18 (0.04)	0.03 (0.01)	0.03 (0.02)	0.03 (0.01)
β_z	1.38 (0.35)	1.20 (0.02)	1.00 (0.41)	1.11 (0.08)	1.15 (0.08)
β_r	0.19 (0.03)	0.11 (0.07)	0.18 (0.06)	0.16 (0.05)	0.15 (0.04)
m_∞ (%)	30.83 (3.17)	30.98 (1.32)	14.31 (0.86)	15.68 (0.63)	18.31 (1.50)

Standard deviations are given within parentheses.

8 h for the LDS composites compared with 50–60 h for the HDS-composites for composites of the same thickness (3 mm). The more hydrophilic LDS matrix evidently showed faster water uptake and reached equilibrium at an earlier stage. In addition, the rougher surface with areas of exposed fibres in the LDS composites as shown in Fig. 1a could contribute to this difference.

Ma et al. [29] studied the impact of fibre content on water uptake in thermoplastic starch composites under different levels of relative humidity and concluded that a greater fibre content is expected to lead to lower water absorption. The influence of fibre content on the water adsorption in the LDS and HDS-composites is shown in Table 2. An increase of fibre content in HDS-composites even enhanced the moisture absorption. In this case, the fibres evidently absorb more moisture than the matrix, unlike the results of Ma et al. [29]. This implies a clear hydrophobization of the starch matrix modified with a high degree of substitution. However, only performing the water absorption under similar test conditions with comparable levels of relative humidity enables a reliable comparison of the results.

The degree of swelling was evidently much higher for LDS composites (Table 2, and Figs. 4 and 5). LDS and HDS-composites exhibited a larger expansion in thickness direction than in the diameter direction. The hot press process results in an in-plane random fibre orientation distribution. The generally high stiffness and low hygroexpansion in the axial direction of the fibres thus inhibit the in-plane expansion along the diameter of the disk-shaped specimens (see e.g. Neagu et al. [30]).

3.3. Mechanical properties

The data obtained from the three-point bending tests were reduced to Young's modulus and tensile strength in dry reference state (conditioned at 60–70% relative humidity, at 25 °C) and for wet saturated samples immersed into water. These values are presented in Table 3. The in-plane and out-of-plane directions are shown schematically in Fig. 6.

The results presented in Table 3, and visualized with diagrams in Figs. 7–9 show some interesting trends. The dry samples (i.e. not immersed into water) were very strong and exhibited extremely high Young's modulus and strength values. Even the unreinforced LDS and HDS-samples showed superior values to corresponding fibre reinforced thermoplastic starches reported in the literature [31]. The crosslinking thus improves the mechanical properties of the starch and its fibre composites. There was a visible discrepancy between the stiffness and strength of unreinforced LDS and the HDS-samples, however the impact of a higher crosslinking is more readily seen in the results of test samples in wet conditions. Though, it is clear that moisture uptake significantly reduces the strength and stiffness, particularly for the LDS composites. The mechanical properties and the structural integrity are further improved by addition of reinforcing wood fibres. Both stiffness and strength increased with increasing fibre content. It is notable that the strength of wet-samples of HDS-60 exceeds the dry unreinforced HDS which is not the case with LDS composites. The benefits on the mechanical properties of starch of a higher degree of cross-linking together with the addition of reinforcing wood fibres are evident. No particular trend of out-of-plane vs. in-plane strengths was found.

Table 3
Young's modulus and ultimate strength in three-point bending of LDS and HDS starch with various fibre contents in wet conditions after saturation in water and at dry conditions

Property (unit)		LDS matrix composite Fibre content (w%)			HDS matrix composite Fibre content (w%)			
		0	40	60	0	40	60	70
Young's modulus (MPa)	Dry	313 (176)	2285 (952)	2823 (415)	359 (46)	2875 (91)	3130 (1257)	3777 (544)
	Wet			138 (86)			428 (131)	
In-plane Strength (MPa)	Dry	13 (3)	56 (10)	59 (4)	15 (3)	77 (9)	90 (42)	146 (14)
	Wet			4 (3)			26 (5)	
Out-of-plane Strength (MPa)	Dry	13 (3)	66 (6)	74 (9)	15 (3)	77 (10)	80 (4)	135 (6)
	Wet			5 (3)			20 (10)	

Standard deviations in parentheses.

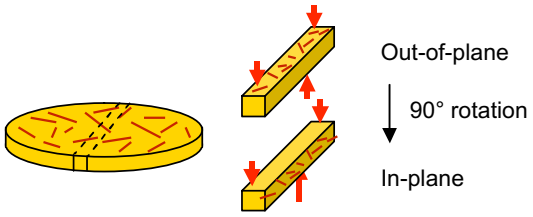

Fig. 6. Test directions in three-point bending of the composite disks with in-plane random fibre orientation distribution.

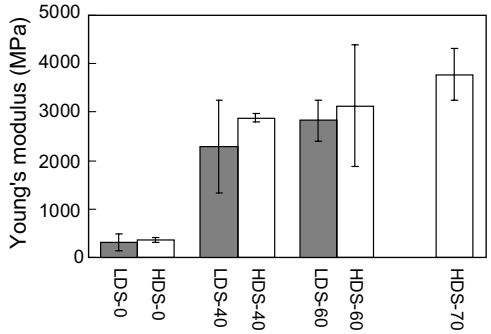

Fig. 7. In-plane Young's modulus of thermoset starch composites. The error bars indicate standard deviations.

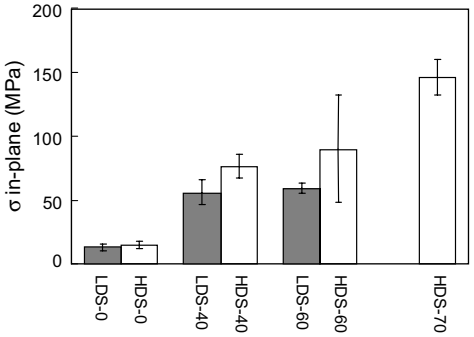

Fig. 8. In-plane strength in three-point bending of thermoset starch composites. The error bars indicate standard deviations.

3.4. Damage mechanisms

The damage mechanisms are shown in the sequence of micrographs during three-point bending in Fig. 10. It can be seen that the crack path becomes more tortuous with the addition of fibres. This is an energy absorbing mechanism which generally implies fibre pull-out and fibre breakage. Concomitantly, the strength values in Table 3 are higher for composites with higher fibre content. The neat HDS matrix shows a planar brittle failure. The HDS-composites show straighter cracks than the LDS matrix, which is indicative of a strong fibre–matrix bond and efficient stress transfer in the matrix. The out-of-plane loading shows a more winding crack path due to the difference in fibre orientation distribution.

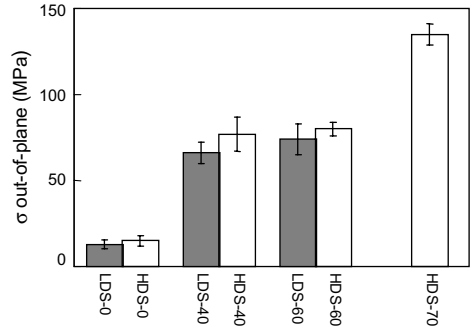

Fig. 9. In-plane strength in three-point bending of thermoset starch composites. The error bars indicate standard deviations.

The fracture of the LDS-60 with higher fibre content showed more pullout in both test directions. The HDS matrix was not that sensitive to an increased fibre content and the HDS-60 and -70 composites behaved like the HDS-40 composites with lower fibre content showing only a limited fibre pull-out tendency. The LDS matrix would be expected to interact better with the fibres as there are more available sites of hydrogen bonding due to the lower degree of substitution. However, the HDS matrix is more hydrophobic due to its higher degree of substitution and this enabled a better dispersion of the hydrophobic crosslinker which probably have resulted in a more homogeneous curing through out the matrix. The HDS also benefits from higher substitution in terms of improved internal plasticizing which obviously reduces the melt viscosity of the starch matrix and provides a more homogeneous matrix distribution.

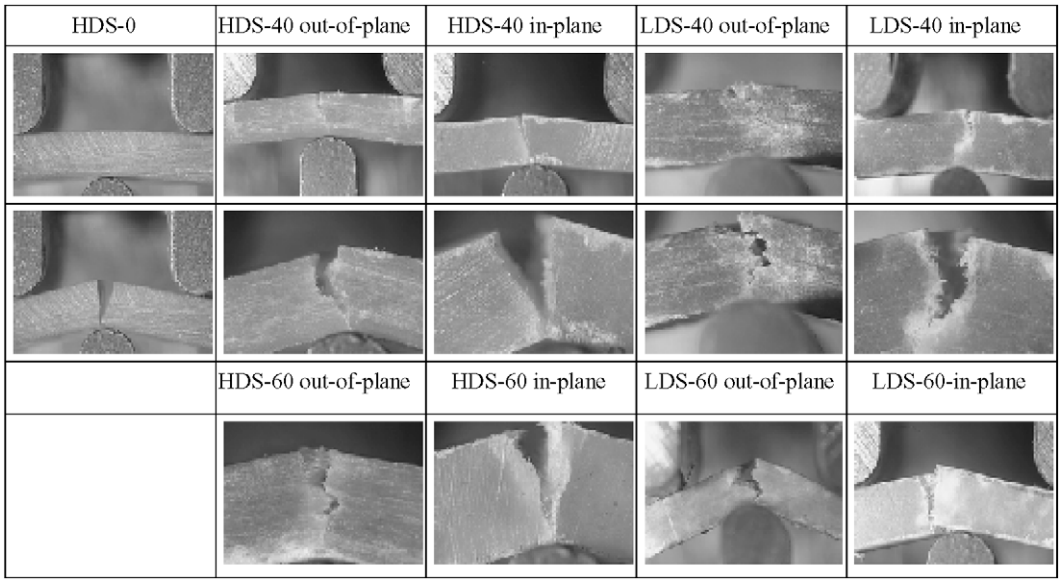

Fig. 10. Sequences of in situ micrographs during three-point bending of the 3 mm thick LDS and HDS-composite samples in dry conditions.

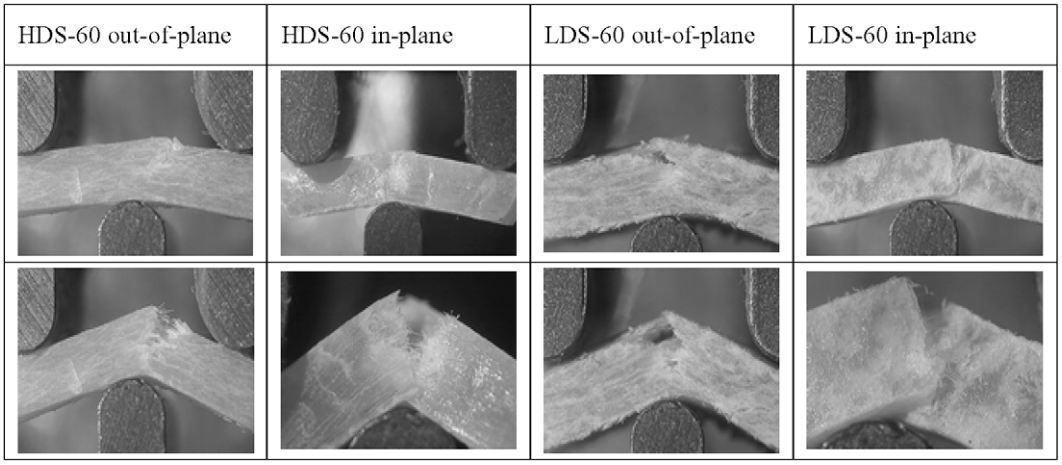

Fig. 11. Sequences of in situ micrographs during three-point bending of the 3 mm thick LDS and HDS-composite samples in wet conditions after saturation in water.

For the wet samples in Fig. 11, extensive fibre pull-out is observed in particular for the more hygrophilic LDS matrix composite. In this case the fibre–matrix interface has become too weak to carry any load, and the fibres are easily pull-out in the crack wake.

4. Conclusions

Thermoset composites of allylglycidyl-ether modified starch, various amounts of wood fiber and ethylene glycol dimethacrylate as crosslinker has been tested for their hygromechanical properties. The presence of bleached softwood fibre with an aspect ratio of up to 100 readily works as reinforcement, even in very high quantities up to 70 wt%, which significantly increases the Young's modulus and tensile strength. The measured strengths are an order of magnitude higher than values reported for related biocomposites with thermoplastic biopolymer matrix systems. The fibres were well distributed in the high degree substitution-matrix HDS and excellent wetting between the fibres and the HDS starch was observed. The low degree substitution-matrix (LDS) exhibits also good matrix–fibre contact, though it produced composites with heterogeneous surface properties seen as fibres not covered by the matrix. The composite water sensitivity was noticeably reduced by higher AGE content in the HDS matrix. Overall, the more hydrophobic high degree substitution-matrix (HDS) resulted in superior mechanical properties.

References

[1] Bledzki AK, Gassan J. Composites reinforced with cellulose based fibres. Prog Polym Sci 1999;24(2):221–74.
[2] Mohanty AK, Misra M, Hinrichsen G. Biofibres, biodegradable polymers and biocomposites. An overview. Macromol Mater Eng 2000;276/277:1–24.

[3] Mishra S, Mohanty AK, Drzal LT, Misra M, Hinrichsen G. A review on pineapple leaf fibers, sisal fibers and their biocomposites. Macromol Mater Eng 2004;289(11):955–74.
[4] Liu W, Misra M, Askeland P, Drzal LT, Mohanty AK. Green composites from soy based plastic and pineapple leaf fiber: fabrication and properties evaluation. Polymer 2005;46(8):2710–21.
[5] Riedel U, Nickel J. Natural fibre-reinforced biopolymers as construction materials. New discoveries. Angewandte Makromolekulare Chemie 1999;272:34–40.
[6] Mohanty AK, Tummala P, Liu W, Misra M, Mulukutla PV, Drzal LT. Injection molded biocomposites from soy protein based bioplastic and short industrial hemp fiber. J Polym Environ 2005;13(3): 279–85.
[7] Huda MS, Drzal LT, Misra M, Mohanty AK, Williams K, Mielewski DF. A study on biocomposites from recycled newspaper fiber and poly(lactic acid). Ind Eng Chem Res 2005;44(15):5593–601.
[8] Cyras VP, Vallo C, Kenny JM, Vazquez A. Effect of chemical treatment on the mechanical properties of starch-based blends reinforced with sisal fiber. J Compos Mater 2004;38(16):1387–99.
[9] Liu WJ, Mohanty AK, Askeland P, Drzal LT, Misra M. Influence of fiber surface treatment on properties of Indian grass fiber reinforced soy protein based biocomposites. Polymer 2004;45(22):7589–96.
[10] Shibata M, Ozawa K, Teramoto N, Yosomiya R, Takeishi H. Biocomposites made from short abaca fiber and biodegradable polyesters. Macromol Mater Eng 2003;288(1):35–43.
[11] Wibowo AC, Mohanty AK, Misra M, Drzal LT. Chopped industrial hemp fiber reinforced cellulosic plastic biocomposites: thermomechanical and morphological properties. Ind Eng Chem Res 2004;43(16):4883–8.
[12] Averous L, Boquillon N. Biocomposites based on plasticized starch: thermal and mechanical behaviors. Carbohyd Polym 2004;56(2): 111–22.
[13] Mohanty AK, Drzal LT, Misra M. Engineered natural fiber reinforced polypropylene composites: Influence of surface modifications and novel powder impregnation processing. J Adhes Sci Technol 2002;16(8):999–1015.
[14] Bien F, Wiege B, Warwel S. Hydrophobic modifaction of starch by alkali-catalyzed addition of 1,2-epoxyalkanes. Starch/Stärke 2001;53(11):555–9.
[15] Mahmut S, Milford AH. Cross-linking starch at various moisture contents by phosphate substitution in an extruder. J Carbohyd Polym 2005;59:541–4.
[16] Chen L, Qiu XY, Deng MX, Hong ZhK, Luo R, Chen XS, et al. The starch grafted poly(L-lactide) and the physical properties of its blending composites. Polymer 2005;46(15):5723–9.
[17] Ge XC, Xu Y, Meng YZ, Li RKY. Thermal and mechanical properties of biodegradable composites of poly(propylene carbonate) and starch-poly(methyl acrylate) graft copolymer. Compos Sci Technol 2005;65(14):2219–25.
[18] Lu YSh, Tighzert Lan, Dole P, Erre D. Preparation and properties of starch thermoplastics modified with waterborne polyurethane from renewable resources. Polymer 2005;46(23):9863–70.
[19] Gaspar M, Benko Z, Dogossy G, Reczey K, Czigany T. Reducing water absorption in compostable starch-based plastics. Polym Degrad Stabil 2005;90(3):563–9.
[20] Avella M, Errico ME, Rimedio R, Sadocco P. Preparation of biodegradable polyesters/high-amylose–starch composites by reactive blending and their characterization. J Appl Poly Sci 2002;83(7): 1432–42.
[21] Smits ALM, Kruiskamp PH, Van Soest JJG, Vliegenthart JFG. Interaction between dry starch and plasticizers glycerol or ethylene glycol, measured by differential scanning calorimetry and solid state NMR spectroscopy. Carbohyd Polym 2003;53(4): 409–16.
[22] Mali S, Grossmann MVE, Garcia MA, Martino MN, Zaritzky NE. Mechanical and thermal properties of yam starch films. Food Hydrocoll 2004;19(1):157–64. Volume Date 2005.
[23] Follain N, Joly C, Dole P, Bliard C. Properties of starch based blends. Part 2. Influence of poly vinyl alcohol addition and photocrosslinking on starch based materials mechanical properties. Carbohyd Polym 2005;60(2):185–92.
[24] (a) Curvelo AAS, de Carvalho AJF, Agnelli JAM. Thermoplastic starch–cellulosic fibers composites: preliminary results. Carbohyd Polym 2001;45(2):183–8;
(b) Avérous L, Fringant C, Moro L. Starch-based biodegradable materials suitable for thermoforming packaging. Starch/Stärke 2001;53:368–71.
[25] Duanmu J, Gamstedt EK, Rosling A. Synthesis and preparation of crosslinked allylglycidyl-ether modified starch-woodfibre composites, Starch/Stärke, submitted for publication.
[26] (a) Mark RE. Cell-wall mechanics of tracheids. New Haven: Yale University Press; 1967;
(b) Kellogg RM, Wangaard FF. Variation in the cell-wall density of wood. Wood Fiber Sci 1969;1:180–204.
[27] Pierron F, Poirette Y, Vautrin A. A novel procedure for identification of 3D moisture diffusion parameters on thick composites: theory, validation and experimental results. J Compos Mater 2002;36(19): 2219–43.
[28] Timoshenko SP, Goodier JN. Theory of elasticity. 2nd ed. McGraw-Hill Book Co; 1970. p. 99–107.
[29] Ma X, Yu J, Kennedy JF. Studies on the properties of natural fibers reinforced composites. Carbohyd Polym 2005;62:19–24.
[30] Neagu RC, Gamstedt EK, Lindström M. Influence of wood-fibre hygroexpansion on the dimensional instability of fibre mats and composites. Compos A 2005;36(6):772–88.
[31] Follain N, Joly C, Dole P, Bliard C. Mechanical properties of starch-based materials. I. Short review and complementary experimental analysis. J Appl Polym Sci 2005;97:1783–94.